On the Summertime Strengthening of the Northern Hemisphere Pacific Sea Level Pressure Anticyclone

SUMANT NIGAM AND STEVEN C. CHAN

Department of Atmospheric and Oceanic Science, University of Maryland, College Park, College Park, Maryland

(Manuscript received 8 November 2007, in final form 27 July 2008)

ABSTRACT

This study revisits the question posed by Hoskins on why the Northern Hemisphere Pacific sea level pressure (SLP) anticyclone is strongest and maximally extended in summer when the Hadley cell descent in the northern subtropics is the weakest. The paradoxical evolution is revisited because anticyclone buildup to the majestic summer structure is gradual, spread evenly over the preceding 4–6 months, and not just confined to the monsoon-onset period, which is interesting, as monsoons are posited to be the cause of the summer vigor of the anticyclone.

Anticyclone buildup is moreover found focused in the extratropics, not the subtropics, where SLP seasonality is shown to be much weaker, generating a related paradox within the context of the Hadley cell's striking seasonality. Showing this seasonality to arise from, and thus represent, remarkable descent variations in the Asian monsoon sector, but not over the central-eastern ocean basins, leads to the resolution of this paradox.

Evolution of other prominent anticyclones is analyzed to critique the development mechanisms: the Azores high evolves like the Pacific one, but without a monsoon to its immediate west. The Mascarene high evolves differently, peaking in austral winter. Monsoons are not implicated in both cases.

Diagnostic modeling of seasonal circulation *development* in the Pacific sector concludes this inquiry. Of the three forcing regions examined, the Pacific midlatitudes are found to be the most influential, accounting for over two-thirds of the winter-to-summer SLP development in the extratropics (6–8 hPa), with the bulk coming from the abatement of winter storm-track heating and transients. The Asian monsoon contribution (2–3 hPa) is dominant in the Pacific (and Atlantic) subtropics.

The modeling results resonate with observational findings and attest to the demise of winter storm tracks as the principal cause of the summer vigor of the Pacific anticyclone.

1. Introduction

Subtropical sea level pressure anticyclones—majestic semipermanent features over the northern and southern oceans—are an integral element of the atmospheric general circulation: their clockwise (in the Northern Hemisphere) near-surface flow connects the tropical trade wind regime with the midlatitude westerly belt, influencing both. Thermodynamically, the anticyclones reside between the intense convection zones in the deep tropics and the midlatitude storm tracks that extend from the eastern coasts of the continents to the mid-basins, especially in winter. The Northern Hemisphere anticyclones extend well into the midlatitudes in summer, when they occupy close to 50% of the Western Hemisphere surface.[1]

The expansive anticyclones apparently contributed to the naming of the Pacific Ocean and the circumnavigation of the earth. Sailing under the Spanish flag, Ferdinand Magellan entered the South Pacific on 28 November 1521 in his quest to find a westward route to the Spice Islands.[2] Interestingly, Magellan's entry was at a time of the year when the regional sea level pressure is

Corresponding author address: Sumant Nigam, University of Maryland, College Park, 3419 Computer and Space Sciences Bldg., College Park, MD 20742-2425.
E-mail: nigam@atmos.umd.edu

[1] The "subtropical" reference of the anticyclones is, to some degree, at odds with respect to their summer structure, which exhibits robust amplitude in the midlatitudes.

[2] Magellan had earlier visited India in 1505 under Portuguese command taking the eastward route through the Cape of Good Hope and then again in 1508, taking part in battles along the Malabar coast, which lead to Portuguese supremacy over the Indian Ocean. Maritime and economic rivalry lead the Spanish to seek a westward route to the Spice Islands, using Magellan's proven navigational skills.

DOI: 10.1175/2008JCLI2322.1

at its seasonal peak (see Fig. 7). As high pressure is synonymous with fair weather, Magellan found calm seas in the initial leg of his Pacific voyage, which took him northwestward across the expansive subtropical anticyclone in the southeastern basin[3]—in contrast with the stormy conditions encountered in his earlier transit through the southwestern Atlantic and the Straits of Tierra del Fuego. The seasonal timing and track of Magellan's pioneering voyage thus presented him with a striking contrast in sea states, leading to his naming of the *Mare del Zur* (the South Sea, as the Pacific was called then) as the *Mare Pacificum* (Peterson 2007).

The canonical explanation for the existence of the subtropical anticyclones, or at least of the surface high pressure belt in the subtropics, is the descent in the poleward branch of the meridionally overturning Hadley cell. That this belt should consists of separate anticyclones and intervening cols (a relative low pressure region), rather than uniform high pressure, was first emphasized by Bergeron (1930) within the context of airmass and frontal development. Bjerknes (1935) argued for such a belt structure from stability considerations and discussed the organization of ascending and descending regions.[4] The subtropical descent is, of course, associated with deserts, both continental and oceanic, and provides unique and critical pathways for radiative cooling of the tropics (''radiator fins''; Pierrehumbert 1995).

The subtropical anticyclones interact with the underlying oceans as well, and not just by suppressing precipitation along their eastern/southeastern flanks (i.e., through salinity impacts): the clockwise circulation over the northern Pacific, for instance, influences the gyre-scale circulation through the wind stress curl as well as the SSTs along the California coast from coastal upwelling. The colder SSTs and resulting near-surface coolness coupled with the warming of the lower troposphere from adiabatic descent leads to static stability enhancement (e.g., trade inversion) and, in turn, extensive low-level cloudiness with significant radiative impacts in the very regions of suppressed precipitation!

Following Bjerknes's analysis, several hypotheses have been put forward to account for the subtropical anticyclones, including monsoon heating to the east and the west of the anticyclones. The role of eastward heating was noted in a seminal paper by Hoskins (1996, transcript of the 1995 Bernhard Haurwitz Memorial Lecture of the American Meteorological Society), who discussed the forcing of anticyclones in the context of large seasonal fluctuations in their strength and expanse. Hoskins argued that latent heat released over the neighboring landmasses to the east during the summer advance of the continental monsoon into the subtropics generates a Rossby wave response to the northwest of monsoon heating, with the related descent (and orographic interaction) contributing to anticyclone development, especially in the eastern basin.

A strong case for both eastward and westward monsoon heating in forcing the Northern Hemisphere (NH) summer anticyclones, especially the one in the Pacific, was made by Rodwell and Hoskins (2001) from modeling the response of observationally constrained diabatic heating [diagnosed residually from the 15-yr European Centre for Medium-Range Weather Forecasts (ECMWF) Re-Analysis (ERA-15)] through initial-value integrations of a nonlinear, primitive equation model. Ting (1994) had recognized the importance of both heatings, especially, the Indian monsoon heating, in anticyclone forcing earlier (see her Fig. 13), albeit within the more general context of diagnostic modeling of the summertime circulation.[5] The importance of westward heating was also shown by Chen et al. (2001), via a quasigeostrophic modeling analysis. Seager et al. (2003) suggested that the summer strength of the Pacific anticyclone is, secondarily, due to local air–sea interactions at the far ends of the basin, which lead to zonal SST variations, and, in turn, the modulation of the heating distribution, which is consequential.

The influence of local diabatic heating on the summer anticyclone was also assessed by Rodwell and Hoskins (2001), who found low-level diabatic cooling in the northeastern Pacific to be influential. Since this cooling is, in part, due to the longwave emission from stratus cloud tops, it depends on the large-scale adiabatic descent over the anticyclone's eastern/southeastern flank

[3] Antonio Pigafetta accompanied Magellan and survived the circumnavigation to write an account. The open sea they crossed, he wrote, ''was well named Pacific, for during this same time we met with no storm'' (Peterson 2005).

[4] See chapter III (Production and Transformation of Air Masses) in Petterssen's (1940) book titled *Weather Analysis and Forecasting* for a brief English language discussion of these papers.

[5] Ting analyzed the summertime circulation generated by the Geophysical Fluid Dynamics Laboratory's (GFDL) GCM, using a steady-state, linear, primitive equation model. The assessment of the influence of various monsoon heatings is insightful, but some caution is called for given the significantly stronger summertime stationary waves in this GCM; these waves are a factor of ~2 larger in the lower troposphere (see Figs. 1b and 2b in Ting's paper). This is consistent with the stronger diabatic heating in the GCM; for example, heating in the Indian and western Pacific sector is larger by a factor of 1.5–2.0 vis-à-vis the observationally constrained heating estimate (cf. Fig. 2 in Rodwell and Hoskins 2001).

for sustenance. As such, its influence, while considerable, is of a feedback, rather than a causative, nature.[6]

It is noteworthy that the above-cited studies focus on modeling the summer circulation—not circulation development, which is the pertinent modeling target in the context of the summer peaking of the anticyclone's strength and expanse. The origin of the winter-to-summer change in circulation features, for instance, depends as much on the winter forcing as the summer one, especially in the case of gradual development. Modeling either circulation should, nonetheless, provide some insights into the origin of circulation evolution, as the above-cited studies sought to do from modeling of the summertime flow.

The monsoon heating, which is intrinsically seasonal, could well account for the summer vigor of the anticyclones. The continental heating to the east and west of the Pacific anticyclone, for example, is undoubtedly influential in the above modeling studies. The modeled monsoon influence (especially the Asian monsoon) however extends over large parts of the tropical and subtropical Pacific (e.g., central/eastern basin) where seasonal sea level pressure development is weak in nature (a section 3 finding). The monsoons may thus not be the only significant influence in the region or their impact could replace another that abates from winter to summer. Observational analysis, described in section 3, moreover shows the largest winter-to-summer change in Pacific sea level pressure to occur in the middle- and high-latitude basin.[7] Together, these observational features suggest that the reasons for the summer robustness of the NH anticyclone may not all be known.

This observationally rooted study revisits the question posed by E. Sarachik (Hoskins 1996) on why the NH anticyclones are strongest and maximally extended in summer when the Hadley cell descent in northern latitudes is the weakest. The study begins with the examination of seasonal sea level pressure development in the Pacific basin. The characterization of annual variability, especially the finding of an incremental buildup of the anticyclone during spring and summer months, raises the specter of an incomplete understanding of the involved processes, necessitating a revisit of the anticyclone development question.

The study seeks to critique the mechanisms advanced for the impressive waxing and waning of the NH anticyclones, especially the Pacific one, from both observational and diagnostic modeling analyses. Intercomparison of seasonal sea level pressure (SLP) variability in the Pacific and Atlantic basins (section 3), analysis of the monthly evolution of upper-tropospheric descent in the northern subtropics (section 4), examination of the seasonal structure of the 200-hPa divergent circulation (section 5), and intercomparison of annual SLP variability in the Northern and Southern Hemispheres (section 6) all contribute to the observational assessment. The modeling analysis begins in section 7, which describes the diagnostic model, its forcing datasets, and its performance. A dynamical diagnosis of winter-to-summer SLP development, especially the contribution of regional forcing onsets and abatements, is presented in section 8. Concluding remarks follow in section 9.

2. Datasets

The ECMWF global reanalysis data provide the necessary atmospheric variables for the present analysis. The 40-yr ECMWF Re-Analysis (ERA-40; Uppala et al. 2005) spans September 1957–August 2002 and is locally available on a 2.5° grid and 23 levels in the vertical. The seasonal evolution is analyzed using the calendar month climatology for the satellite era (1979–2001).

Monthly precipitation data came from the Climate Prediction Center's (CPC) Merged Analysis of Precipitation (CMAP; Xie and Arkin 1997). The CMAP precipitation data are also available on a 2.5° grid, and the observation-only CMAP product (CMAP-2) was used.

3. Seasonal variability of Pacific sea level pressure

The monthly distribution of SLP and precipitation is shown in Fig. 1 for the first half of the calendar year. The most remarkable change in SLP is the winter-to-summer abatement and the northward retreat of the Aleutian low and its replacement by high pressure, especially in the central and eastern basins, which results in a majestic anticyclone in July. The synchronicity of these changes is noteworthy. At its peak, the anticyclone is centered in the 35°–40°N band and extends over most of the extratropical basin. In contrast, the anticyclone is quite weak in January when it is confined to the far eastern basin. The January-to-July change in core

[6] A similar feedback from stratus cloud-top cooling fosters the annual warm-to-cold SST transition in the eastern tropical Pacific in the modeling analysis of Nigam (1997), who argued that dynamic feedback of cloud-top longwave cooling in coastal upwelling regions is more rapid than the thermodynamic feedback from stratus shading.

[7] Eastern Hemisphere monsoons are found to be influential in this region too in the cited modeling studies but their influence was generated from an overly extended diabatic heat source in most cases: up to 150°E–170°W to the east and 60°N, making separation of local and remote effects difficult.

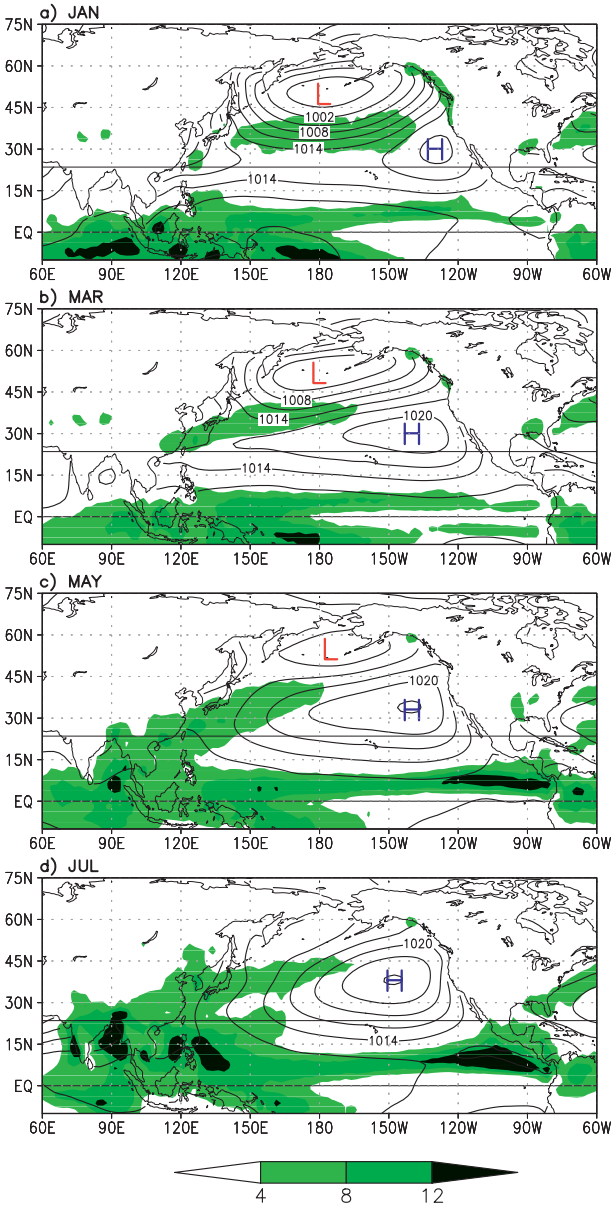

FIG. 1. Cold-to-warm season evolution of SLP (contoured) and precipitation (shaded) in the 1979–2001 period monthly climatology. SLP is taken from ERA-40 and precipitation from CMAP-2 for (a) January, (b) March, (c) May, and (d) July. SLP is contoured every 3.0 hPa, and precipitation shaded at 4.0 mm day^{-1} intervals, beginning at 4.0 mm day^{-1}, as indicated by the color bar. Major SLP centers (the Pacific high and the Aleutian low) are marked. The tropic of Cancer (drawn) provides positional reference during seasonal evolution.

pressure is ~6 hPa, but substantially larger SLP change occurs in the northern basin (as shown later).

The concurrent monthly precipitation, which reflects the vertically averaged latent heating, is depicted in the same panels of Fig. 1 for context. Winter precipitation occurs along the southern flank of the Aleutian low, which forms the axis of the jet and winter storm tracks, as well as along its eastern/southeastern flank where the large-scale vorticity balance—the Sverdrup balance—implies low-level convergence and, thus, ascending motion and rainfall, that is, the winter rainy season in the Pacific Northwest. [See Nigam and Ruiz-Barradas (2006) for more discussion of this subject, including contribution of the transient moisture fluxes to winter rainfall.] The Aleutian low is, of course, itself forced in good measure by the storm track diabatic heating and transients (cf. Fig. 9b in Hoskins and Valdes 1990 and Fig. 11e in this paper). With the onset of spring and summer, the Aleutian low retreats northward and the related precipitation impacts diminish, vanishing altogether by July when the U.S. west coast is under the influence of descending motions associated with the eastern flank of the anticyclone, that is, California's ''Mediterranean'' summer climate. Farther equatorward, the Asian and American monsoons and the intertropical convergence zone (ITCZ) are fully developed by July; note the double-ITCZ structure in March.

The location and spatial extent of the SLP anticyclone are tracked in Fig. 2 by monitoring the movement of the 1020-hPa SLP contour in alternate months, beginning with January (denoted 1). The tracking of curves labeled 1–7 indicates that anticyclone development during spring and summer primarily involves the northward advance of the high pressure region; the westward advance occurring earlier (late winter). The most striking feature however is the little change in the subtropical basin, as evident from the overlap of the March–July (3, 5, and 7) isobars.

The case for the absence of significant change in seasonal SLP in the tropical and subtropical basin is directly made in Fig. 3, which displays the SLP change over 2-month periods, along with the tropic of Cancer as a positional reference. The largest 2-month change in the build-up phase is between January and March (~8 hPa in the top panel in Fig. 3) when SLP increases over the extratropical Pacific in the Aleutian low longitudes (i.e., the central basin; cf. Fig. 1a). Meridionally, this SLP change is in quadrature with the Aleutian low, so that the low is confined to the northern basin in March. It is noteworthy that the largest seasonal increase in SLP in the tropics–subtropics (e.g., the 15°–30°N belt), of up to 4 hPa, occurs in this period. The subsequent March–May change (Fig. 3b) is focused in the midlatitudes but with some preference for the western basin. The following May–July SLP change is more like the January–March change in the midlatitudes but with the tropics and subtropics exhibiting a 1–2-hPa reduction in SLP! The reduction is moreover concentrated in the western and eastern basins, adjacent to the warm

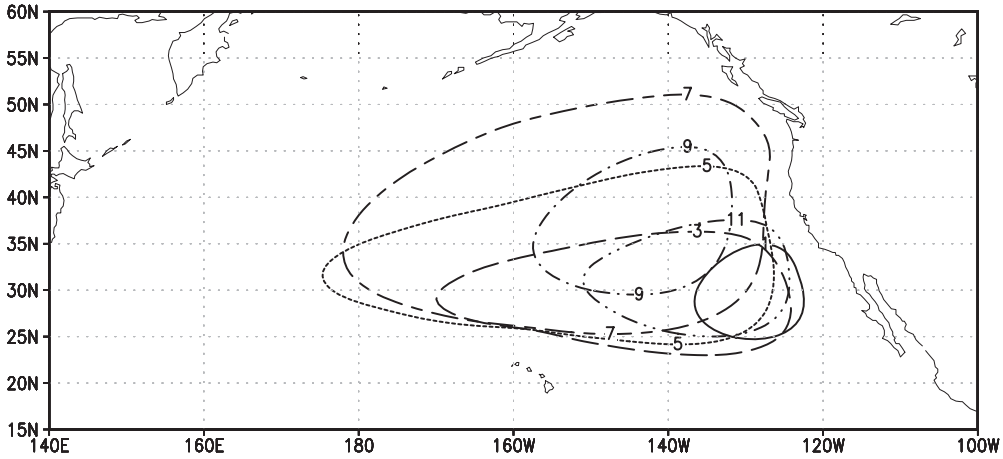

FIG. 2. Monthly evolution of the Pacific SLP anticyclone. The 1020-hPa isobar in the climatological (1979–2001) SLP field is tracked at 2-month intervals, beginning in January. Isobars are labeled by the calendar month number; for example, January is 1 and November is 11. The cold-to-warm season development essentially consists of a westward and northward expansion of the anticyclone.

continents, and is consistent with the reach of the continental monsoons, especially the Asian one to the west.

The lower panels in Fig. 3 mirror the development portrayed in upper panels, except for the sign. Cyclonic development begins in early autumn and proceeds with increasing vigor with the advent of winter. This development is also focused in the northern midlatitude basin, but for the presence of continental influences in the subtropics in autumn, which mirror the springtime change. Seasonal SLP variability in the Pacific is evidently annual in nature, in contrast with seasonal variability in the tropical–subtropical Atlantic (not shown), where it is more semiannual.[8]

The May–July SLP reduction, albeit modest but nonetheless occurring in the monsoon onset period, is seemingly at odds with the modeling analyses indicating a role for Asian monsoon heating in anticyclone development. These studies show that Asian monsoon heating leads to a positive (and not negative) SLP response in the Pacific tropics and extratropics (Fig. 12b in Ting 1994; Fig. 9a in Chen at al. 2001).[9] Ting's analysis (Fig. 12) also shows the low-level response over the Pacific to be both augmented and offset by heating in other sectors. The possibility that the monsoon heating's influence over the Pacific is offset by other thermal and/or mechanical forcings in nature was raised in the introduction.

The seasonal cycle of Pacific SLP is compactly shown atop its annual-mean distribution in Fig. 4 (top panel). The amplitude and phase of the annual harmonic are denoted by the length and direction of the plotted arrows; arrows pointing due north (locally) indicate a summer maximum and a winter minimum. The annual-mean distribution consists of a high in the eastern subtropical basin and a low in the northern basin, reflecting some persistence of the summer and winter features in these regions, respectively.

More striking though is the distribution of the annual variability, which is weaker than 1 hPa in amplitude (the vector-plotting threshold) in the entire tropics and subtropics, excluding the far western and eastern coastal sectors where the influence of continental monsoons is manifest, with lower SLP in July. Robust annual variability is however found in the middle and high latitudes, with the amplitudes being particularly large northward of 35°N in the central and eastern basins. The structure of the annual SLP variability over the Pacific basin raises the following interesting questions:

- Why is the seasonal SLP variability in the Pacific subtropics so weak despite the significant winter-to-summer variation of the Hadley cell descent in these latitudes? The question is similar to the one posed by Hoskins (1996), except that it is the weak seasonal

[8] The Atlantic sector (100°–60°W) is more responsive to the twice-yearly overhead position of the sun at the tropic of Cancer because of the presence of land in this sector (eastern Mexico, FL, and Cuba, among others), with low SLP following the equinoxes within a month, at monthly resolution.

[9] Rodwell and Hoskins' (2001) modeling analysis does not show the low-level streamfunction (or SLP) forced by Asian monsoon heating alone. The closest is the response of the orography and Asian monsoon heating (Fig. 8b), with positive SLP in the Pacific tropics and extratropics in July. Their Asian heating box (10°S–60°N, 60°–150°E) also seems too inclusive as the western North Pacific monsoon is within the box.

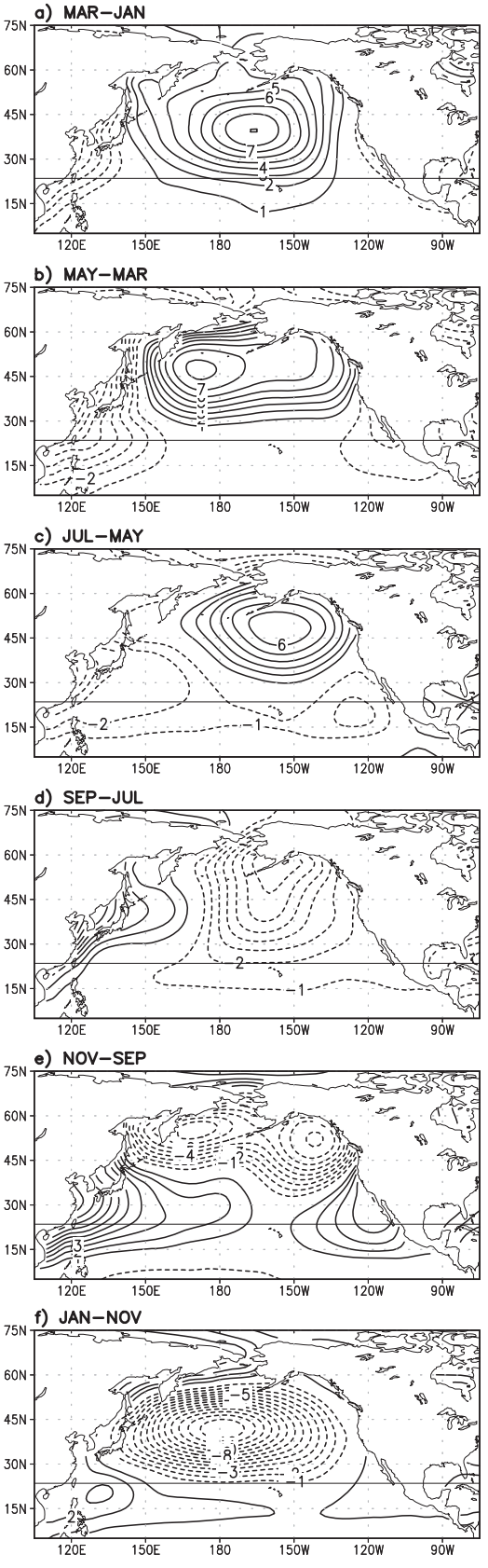

signal in the tropics–subtropics (cf. Figs. 2–4), rather than perceptions of a counterintuitive one (cf. Hoskins 1996), that is enigmatic.

- How significant and extensive is the influence of continental monsoons on Pacific SLP, especially in the northern basin, which exhibits striking, albeit gradual, development?

Prior to seeking answers from a modeling analysis (section 7), clues are sought in the structure of seasonal SLP variability in the Atlantic basin, which does not have an Asian monsoon equivalent to its west. The annual cycle of the Atlantic SLP is displayed in the bottom panel in Fig. 4 using the same scale and format as earlier to facilitate intercomparison. The annual-mean field consists of a basin-wide anticyclone, called the Azores high (or Bermuda high), which exhibits weak annual variability except at its northern flank.

Annual SLP variability in the Atlantic is, evidently, largest in the northern basin, much as in the Pacific, and quite weak in the tropical and subtropical latitudes of the interior basin, as is also the case in the Pacific. The similarity continues in near-coastal regions where continental influences (and summer low pressures) are manifest in both basins. The correspondence of annual SLP variations in the two basins is striking and remarkable considering that one of them has a powerful monsoon system to its west. The similarity suggests that either having a monsoon to the west of the anticyclone is inconsequential or else the global reach of the Asian summer monsoon is.

4. Evolution of upper-tropospheric descent

The striking winter-to-summer variation of the Hadley cell along with perceptions that such variability typifies seasonal changes across most longitudes are at the core of the conundrum implicit in the first of the above questions. Recent analysis by Dima and Wallace (2003) however shows the Hadley cell's seasonality to be linked with the monsoons, that is, with *regional* circulations forced by summer heating of the continents; in agreement with early views of Hadley cell seasonality (Newell et al. 1972). The analysis shows that the Hadley cell's seasonality is reflective of regionally concentrated, rather than longitudinally widespread, seasonal changes

←

Fig. 3. Pacific SLP *development*, the 2-month change in climatological SLP: (a) January–March, (b) March–May, (c) May–July, (d) July–September, (e) September–November, and (f) November–January. The SLP change is contoured at 1.0-hPa intervals, with solid (dashed) contours indicating positive (negative) development. The tropic of Cancer is again shown for positional reference.

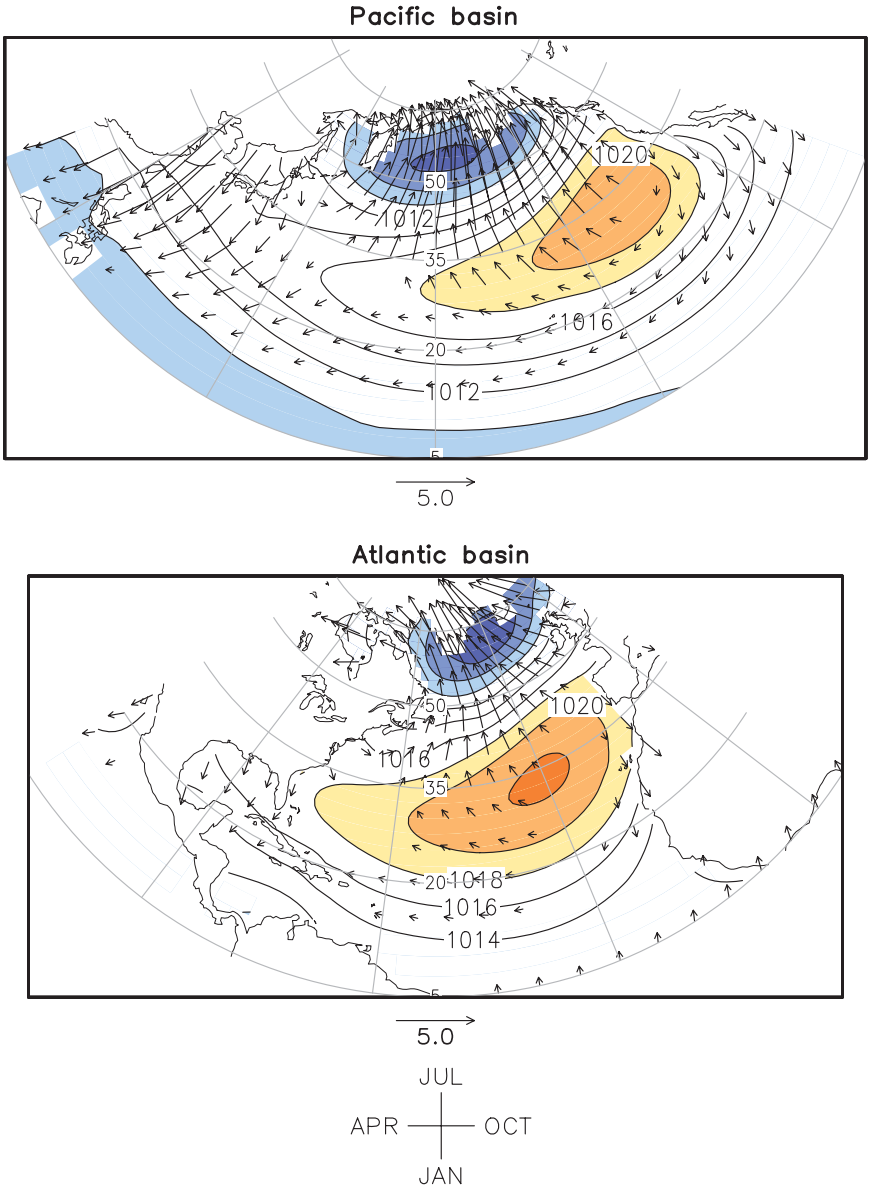

FIG. 4. Annual mean and annual cycle of SLP in the Pacific and Atlantic basins, based on ERA-40 monthly climatology (1979–2001). Annual-mean SLP is contoured at 2.0-hPa intervals, with values above (below) 1018 (1010) hPa shaded. The annual variability is displayed using vectors, with the length denoting amplitude and the direction showing the phase, as indicated above. A *locally* northward pointing vector, for example, indicates maximum (minimum) SLP in July (January). Vectors are not drawn when the variability amplitude is less than 0.5 hPa.

in divergent circulations, correcting flawed perceptions to the contrary.

The Dima–Wallace analysis is supplemented in this section by displays of the monthly evolution of upper-level descent across all longitudes in the northern subtropics, including oceanic midbasins where the SLP variability was found to be weak (Figs. 2–4). The negative of the 300-hPa pressure vertical velocity ($-\omega_{300}$) is plotted in the 15°–25°N band in Fig. 5, with the zonal mean plotted in the adjacent right panel.[10] The band was chosen to fully include the winter and summer descent regions over the Pacific and Atlantic basins (cf. Fig. 6).

The descent is strongest in winter across most longitudes, much as expected; with the zonal-mean change

[10] An upper rather than midtroposphere level was chosen to avoid the below-ground interpolated values, given the presence of high mountains in the northern subtropics.

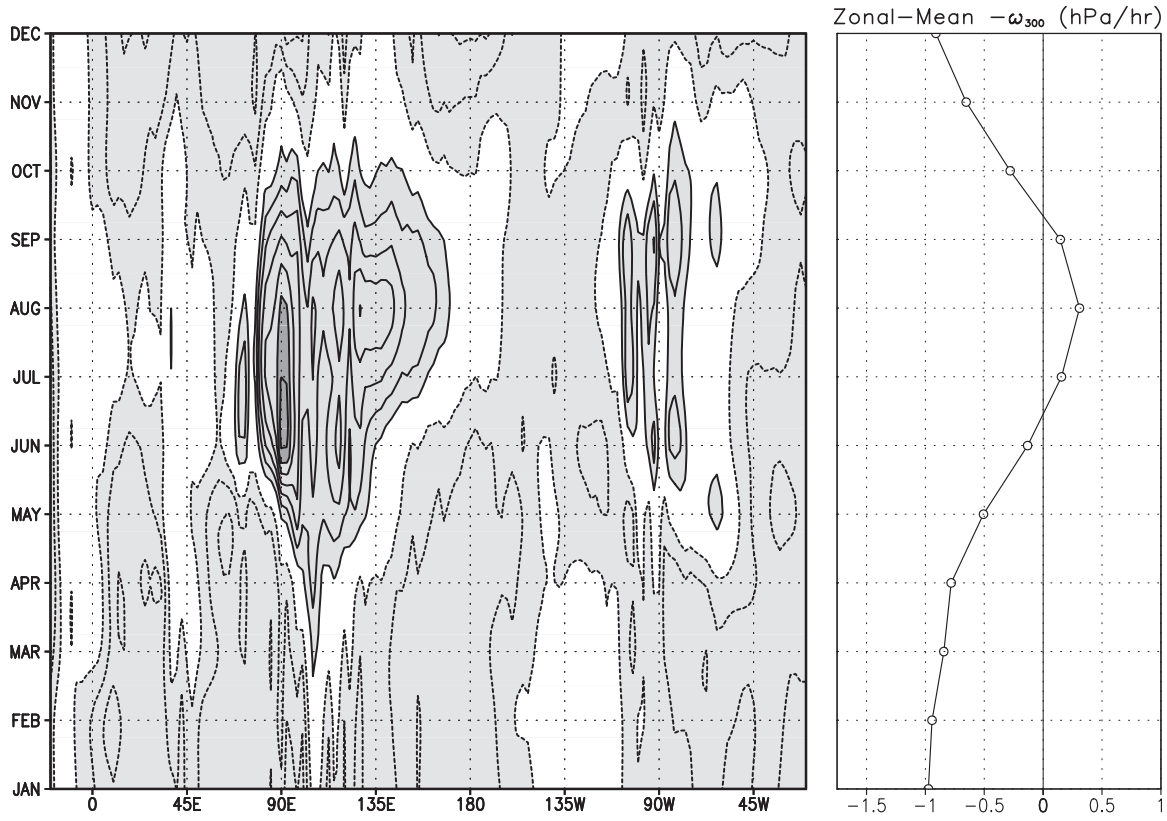

FIG. 5. Monthly evolution of the 300-hPa vertical velocity ($-\omega_{300}$) in the NH subtropics (15°–25°N), based on ERA-40 climatology (1979–2001). (left) The longitudinal distribution and (right) corresponding zonal mean are displayed. Contour interval is 0.5 hPa h^{-1}. Solid (dashed) contours indicate positive (negative) values, and the zero contour is omitted.

(Fig 5., right panel) being representative of winter development in most longitudes. The descent varies little between winter and spring, continuing unabated until late spring in some sectors (e.g., the Sahara desert, and the western-central Pacific and mid-Atlantic basins), that is, during the period of the Hadley cell's transformation from a single-cell winter structure into a more evenly balanced two-cell equinoctial configuration. The zonal-mean descent is clearly impacted by the development of the Asian and North American monsoons in late spring. The monsoon impact in summer is, of course, overwhelming, with strong, deep ascent manifest not only in the Asian and American longitudes but also in the zonal mean, leading to a northward extension of the rising branch (e.g., the *ERA-40 Atlas*; Kållberg et al. 2005) and, thus, a narrowing of the summer cell. Farther to the north (e.g., 25°–30°N), monsoon ascent leads to a reduction in the zonal-mean subsidence, that is, to cell weakening. Monsoons are thus integral to the Hadley cell's seasonality, in both strength and structure, in accord with the results of Dima and Wallace (2003).

In the context of anticyclone development, Fig. 5 shows the upper-level descent over oceanic basins to be weaker in summer, reflecting some influence of the Asian and western North Pacific monsoons. The May–July SLP change in the 15°–25°N latitude band is weakly negative (cf. Fig. 3c), consistent with descent evolution. The conundrum is resolved by first noting that the Hadley cell's striking seasonality is not reflective of seasonal changes across most longitudes, as illustrated by the weak seasonality of the descent over the Pacific and Atlantic midbasins. Positive SLP development in summer is, moreover, focused well to the north of this band, closer to 45°N (cf. Figs. 2–4). As such, there is no discord between weaker subtropical descent and positive SLP development in the midlatitude basin. The disaccord suggested in Hoskins (1996) was based on perceptions of positive SLP development in the subtropics, a development that really occurs in the midlatitude basin, as shown here.

5. Monsoon's influence on Pacific basin descent

The influence of the Asian monsoon on the far-field circulation is difficult to characterize from observational analysis, given the concurrent seasonal evolution of other climate features, for example, ITCZ development

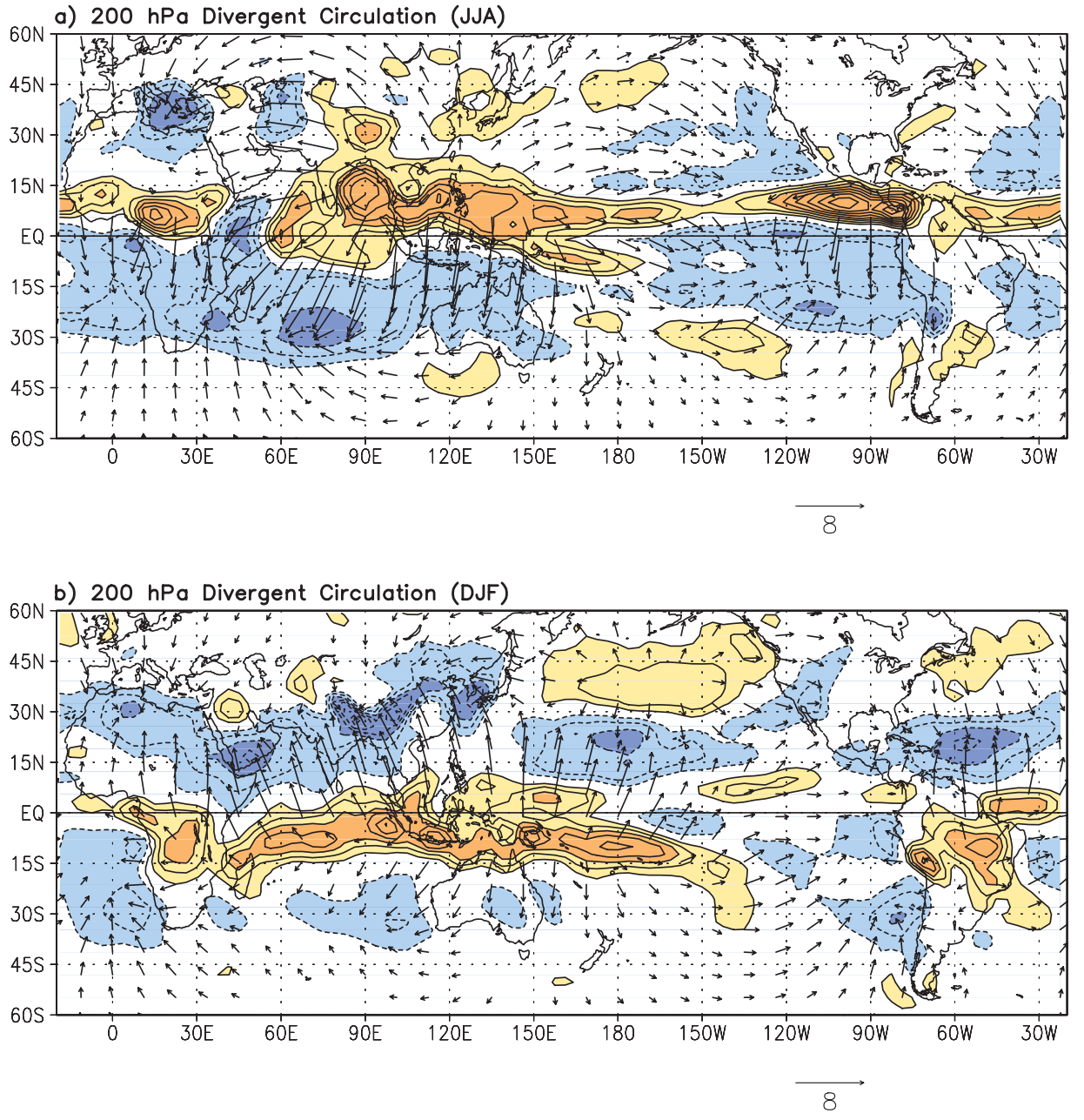

FIG. 6. Divergent circulation in the upper troposphere in (a) June–August and (b) December–February, based on ERA-40 climatology (1979–2001). The 200-hPa divergence is contoured at 10^{-6} s^{-1} intervals and the divergent wind vector is displayed using the indicated scale. Solid (dashed) contours indicate positive (negative) divergence, and the zero contour is omitted.

in the central/eastern equatorial Pacific. The far-field influence consists of both rotational and divergent components, with identification of the former being challenging, observationally, in view of the Rossby wave propagation. The presence of multiple wave sources and refractive index variations (e.g., Karoly and Hoskins 1982; Nigam and Lindzen 1989) can often be confounding. Not surprisingly, the monsoon influence is generally characterized using dynamical models (e.g., Ting 1994; Rodwell and Hoskins 2001).

The monsoon's influence on the upper-level divergent flow is, conceptually, somewhat easier to identify, given the certainty in where this flow originates—in regions of strong monsoonal latent heating. Determination of the flow field however requires knowledge of both the origination (divergent outflow) and termination

(sinking) points, since the surrounding sinking regions are far from uniformly distributed with respect to the outflow core. The sinking regions, it turns out, are determined both by the divergent outflow structure and its rotational response, and the static stability distribution (e.g., Sardeshmukh 1993), that is, from complex dynamical and thermodynamical processes, not all of which are presently well understood.

Notwithstanding such difficulties, the 200-hPa divergent flow is tracked from regions of strong monsoon latent heating in Fig. 6, and the monsoon's influence is taken to extend at least as far as the nearest sinking region. Immediately apparent is the large summer divergent outflow from the Bay of Bengal, the region exhibiting the strongest divergence in the Eastern Hemisphere; the divergent flow is headed mostly northwestward, westward, and southward. The organization of descent (and ascent) to the northwest bears the imprints of Rossby wave propagation, which Rodwell and Hoskins (1996) emphasized in connecting the Asian summer monsoon with the aridity of western Afghanistan and eastern Iran (the first descent region) and the eastern Mediterranean (the second descent region to the northwest). The bulk of the South Asian summer monsoon outflow is however directed southward, to the subtropical southern Indian Ocean, where it leads to the strengthening of the Mascarene high (Krishnamurti and Bhalme 1976). This *regional* meridional overturning is the principal contributor to the austral winter's *zonal-mean* Hadley cell.

The continental monsoon's influence to the east, the focus here in the context of the summer strengthening of the Pacific anticyclone, is comparatively muted in the upper-level descent field, unless one also considers the western North Pacific monsoon when this influence becomes more appreciable, but still modest. That this monsoon system can be assumed to be independent of the Pacific SLP anticyclone is however not clear for it can be argued that this monsoon owes its existence, in part, to the SLP anticyclone itself (Rodwell and Hoskins 2001). This synergism can contribute to anticyclone development, but if the related upper-level descent in Fig. 6 provides any guidance, the western North Pacific monsoon's influence is modest and confined largely to the tropics, except in the far eastern basin where the subtropics are also, to an extent, influenced. Examination of the 200-hPa divergent circulation indicates the Asian monsoon's influence on the upper-level descent over the Pacific to be modest. This, of course, is not a full measure of the monsoon's influence on the Pacific basin, as noted at the beginning of this section. The vorticity dynamics, in particular, vortex stretching in the monsoon latent heat release regions, elicits a substantial rotational response with bearing on the SLP field; a response that is difficult to isolate without the use of models. The related modeling analysis is reported in section 8.

6. Evolution of sea level pressure in the Southern Hemisphere

The seasonal variability of SLP in the hemisphere having significantly less landmass is examined in this section. Reduced landmass in the subpolar Southern Hemisphere (SH) leads to weaker stationary waves and, thus, a more axisymmetric circulation. The storm tracks are more zonal as well, especially in summer (e.g., Hoskins and Hodges 2005). The reduced continentality also leads to weaker monsoons. Such differences make the SH attractive for testing understanding of the atmospheric general circulation.

The annual variability of SLP in the SH is displayed in Fig. 7. The annual-mean field (contoured) is quite zonal in the high latitudes, unlike in the NH. A weak high in the Weddell Sea sector and a zonally diffuse low elsewhere are, nonetheless, discernible. The annual-mean SLP also contains three anticyclones in the SH subtropics, one in each ocean basin, with the Indian Ocean one (the Mascarene high) being the strongest (>1022 hPa).

The annual variability of SLP in the SH is quite distinct from that in the NH, as evident from the distribution and orientation of the annual harmonic arrows in Fig. 7. The annual variability is primarily focused in the tropical–subtropical latitudes, unlike in the NH, where high latitudes are the focus region (cf. Fig. 4). This difference leads to a strikingly different evolution: an equatorward strengthening/expansion of the SH anticyclones as opposed to the poleward development of the NH ones. Phase differences, moreover, lead to different peak-phase timings: austral winter and boreal summer, respectively. What could cause such interhemispheric differences in SLP evolutions?

- *Storm tracks*: The SH storm tracks are located in the high latitudes, close to the Antarctic Circle.[11] As such, they are well separated from the subtropical anticyclones and are, perhaps, less influential. This is unlike the NH where storm tracks are mostly in the midlatitudes (40°–50°N), that is, in proximity to the SLP anticyclones.

[11] The poleward location (~60°S) of the SH storm tracks can be seen in the bandpass-filtered variance of SLP. Compare, for instance, the NH winter (DJF) distribution (Fig. 3a in Hoskins and Valdes 2002) with the SH winter (JJA) one (Fig. 3f in Hoskins and Hodges 2005).

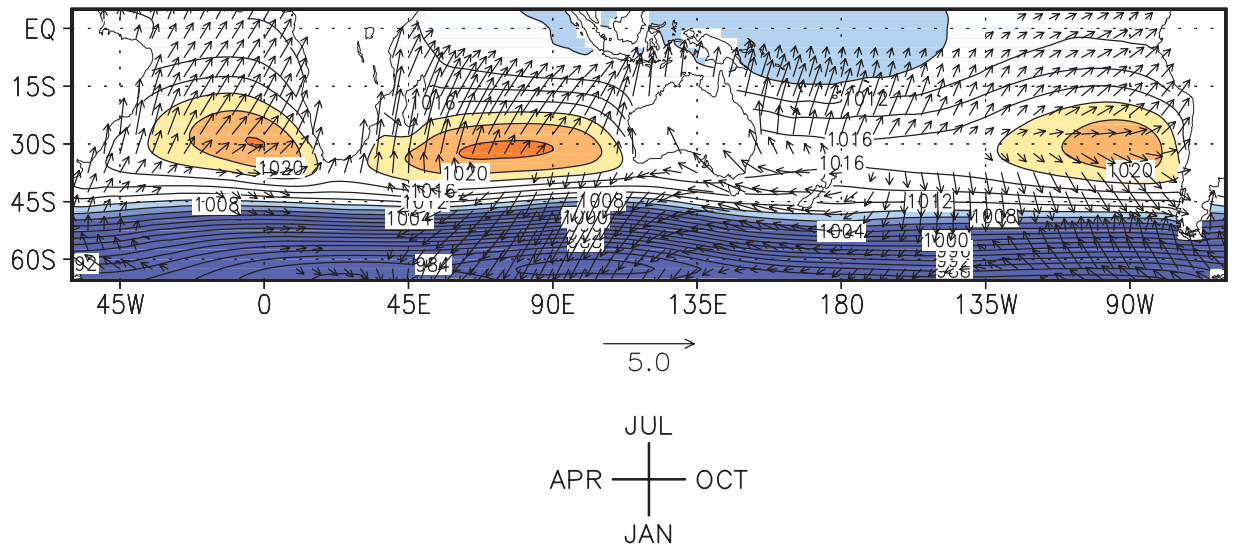

FIG. 7. Annual mean and annual cycle of SLP in the global SH, based on ERA-40 monthly climatology (1979–2001). A *locally* northward pointing vector, for example, indicates maximum SLP in July, as before. Otherwise, as in Fig. 4.

- *Monsoons*: The SH monsoons are weaker, with the monsoon regions located somewhat equatorward, which further reduces their influence (Rodwell and Hoskins 2001). Even so, there is considerable rainfall development over subtropical South America, including Amazonia, from winter (June–August, JJA) to summer (December–January, DJF). Assuming some monsoon influence on downstream SLP development, one would expect a stronger anticyclone in the subtropical South Atlantic in austral summer (DJF).[12] Observations, however, indicate the anticyclone to be stronger in austral winter, as is the one in the Indian Ocean.
- *Hadley descent*: Meridional overturning in the Eastern Hemisphere is the principal contributor to the Hadley cell, including its seasonality (cf. Fig. 6). Descent in the SH tropics–subtropics is strongest in JJA and focused in this sector, as it is related to the Asian–African monsoon outflow. Not surprisingly, this sector's SLP anticyclones are strongest in austral winter.

The evolution of the Southern Hemisphere's SLP anticyclones suggests the following:

- Monsoons do not account for the seasonal strengthening of the anticyclones, which peak in austral winter.
- Storm tracks cannot be implicated either, given their subpolar, and thus distant, location relative to the subtropical anticyclones.
- Hadley cell seasonality can apparently account for the waxing and waning of the SH anticyclones, in accordance with dynamical intuition, which is quite unlike the case in the NH. Reduced interference from storm tracks is, perhaps, the reason for the manifestation of this intuitive link in SH circulation.

7. Diagnostic model, forcing datasets, and performance

A modeling analysis of Pacific circulation and SLP is undertaken using the ERA-40 dataset, with the goal of identifying the regional forcing that leads to the development of key SLP features, including winter-to-summer strengthening/expansion of the anticyclone. This section describes the diagnostic model, along with its forcing datasets, and the model's performance.

a. Diagnostic model

The steady linear primitive equation model solves the σ-coordinate ($=p/p_s$) equations. The equations are linearized about a zonally symmetric basic state, and the model solves for the eddy component (i.e., deviation from the zonal average) of the circulation. The linearized equations are given in Held et al. (1989) and modifications to represent vertical diffusion processes in the planetary boundary layer (PBL) are shown in Nigam (1997). Diffusion coefficients vary in the vertical, decreasing rapidly above 850 hPa, all as $30[1 + \tanh\{10\pi(\sigma - 0.85)\}]$. The modeling of diffusion processes requires specification

[12] A similar dynamical response (e.g., from the Sverdrup vorticity balance) is expected in the SH despite the negative Coriolis parameter, for it appears in both the vortex-stretching term and the geostrophic relationship.

of the boundary conditions: the lower one involving drag coefficients, all set to 1.0×10^{-3}. Inclusion of PBL diffusion precludes the need for low-level Rayleigh dissipation but not Newtonian damping of temperature; the damping coefficient is $(15 \text{ days})^{-1}$ when $\sigma < 0.5$, increasing linearly to $(5 \text{ days})^{-1}$ at the surface. The momentum and thermodynamic equations also include horizontal diffusive mixing, with a constant coefficient of $5 \times 10^5 \text{ m}^2 \text{ s}^{-1}$. The diffusive and Newtonian damping of temperature occur on isobaric surfaces in the model.

The diagnostic model is solved numerically, using the semispectral representation for the horizontal structure: 73 grid points between the two poles ($\Delta\theta = 2.5°$) and zonal Fourier truncation at wavenumber 30. The vertical structure is discretized using 18 full-sigma levels, of which 14 are in the troposphere, including 5 below 850 hPa.

b. Forcing datasets

The zonal-mean zonal and meridional winds, temperature, and surface pressure from ERA-40's 1979–2001 climatology constitute the model's basic state, while orography, 3D diabatic heating, and submonthly transient heat and momentum fluxes (diagnosed from 6-hourly reanalyses), as well as the surface temperature from the same dataset, provide the model forcing. Heating was diagnosed in house from ERA-40's 23-level and 2.5° resolution isobaric reanalyses (Chan and Nigam 2009). The heating was diagnosed as a residual in the thermodynamic equation (e.g., Hoskins et al. 1989; Nigam 1994) using monthly data and submonthly transient fluxes, just as was done earlier for the National Centers for Environmental Prediction–National Center for Atmospheric Research (NCEP–NCAR) and ERA-15 reanalyses in Nigam et al. (2000).

Diagnosed forcing fields are displayed in Fig. 8 to demarcate the regions whose response is analyzed next and for reassurance. The mass-weighted heating averages (surface–125 hPa) in winter and summer are shown in Figs. 8a and 8b, respectively. Well-known features such as the ITCZ, South Pacific convergence zone (SPCZ), Maritime Continent convection, Asian monsoon, midlatitude winter storm tracks, and the eastern subtropical Pacific descent and cooling zones are all in evidence, including their seasonal variations. The ERA-40 heating over the Maritime Continent and the Pacific and Atlantic ITCZs is substantially stronger than that in the NCEP–NCAR reanalysis, by as much as a factor of 2 (Chan and Nigam 2009). Three regions are outlined in the heating distributions: the Asian monsoon sector, the ITCZ+SPCZ, and the Pacific storm tracks.

The storm-track region is, in fact, based on the distribution of the 850-hPa meridional wind variance (Figs. 8c and 8d), which is a commonly used to monitor storm-track activity (e.g., Chang 1993). Winter variance is largest in the central North Pacific and Atlantic basins, with storm-track diabatic heating concentrated to the west of the wind variance maximum.

c. Model performance

A prerequisite for dynamical diagnosis is the diagnostic model's ability to simulate the target field: seasonal SLP *development*, here. If notable development features can be simulated, their origin can be investigated, at least, in a diagnostic (a posteriori) sense. For a meaningful analysis, the model should be required to simulate the individual seasonal circulations as well.[13] The model's performance is assessed in Figs. 9 and 10. In the interest of space, and in order to cover both the lower- and upper-tropospheric circulations, the individual season simulations are assessed using the 200-hPa streamfunction (Fig. 9), while simulation of seasonal *development* (the winter to summer change, i.e., JJA–DJF) is evaluated using SLP (for obvious reasons) in Fig. 10.

The simulated and observed winter streamfunctions (Fig 9., upper panels) compare favorably in terms of amplitude and features, with the possible exceptions of the Eastern Hemisphere trough–ridge system, which is placed ~20° upstream in the simulation, and the weaker ridge over northeast Pacific. The summer streamfunctions (Fig. 9, lower panels) are also in good agreement but the Tibetan anticyclone is a bit stronger and the Pacific midbasin trough marginally weaker but more expansive in the simulation. The individual seasonal simulations are, overall, quite realistic.

The difference between the winter and summer SLP simulations is shown in Fig. 10b, while the related ERA-40 target is shown in Fig. 10a.[14] An intercomparion shows the SLP development to be reasonably simulated, with feature-to-feature correspondence with the observations. Deficiencies include a coastal focus and weaker amplitudes in the Pacific basin (by ~4 hPa). The deficiencies are somewhat more pronounced than those manifest in the upper-level simulation but not surprisingly so. The simulation of SLP is challenging given the influence of the PBL processes and the difficulties in parameterizing the same. (For this reason, SLP is seldom displayed in diagnostic modeling analyses; low-level

[13] Or better yet, their average. The development ($b - a$) and average ($b + a$) are independent states, and a model that simulates both offers prospects for insightful analysis.

[14] The full fields (zonal mean + zonal varying) are subtracted in these panels to avoid differences in the below-ground interpolation schemes from influencing SLP over the open oceans.

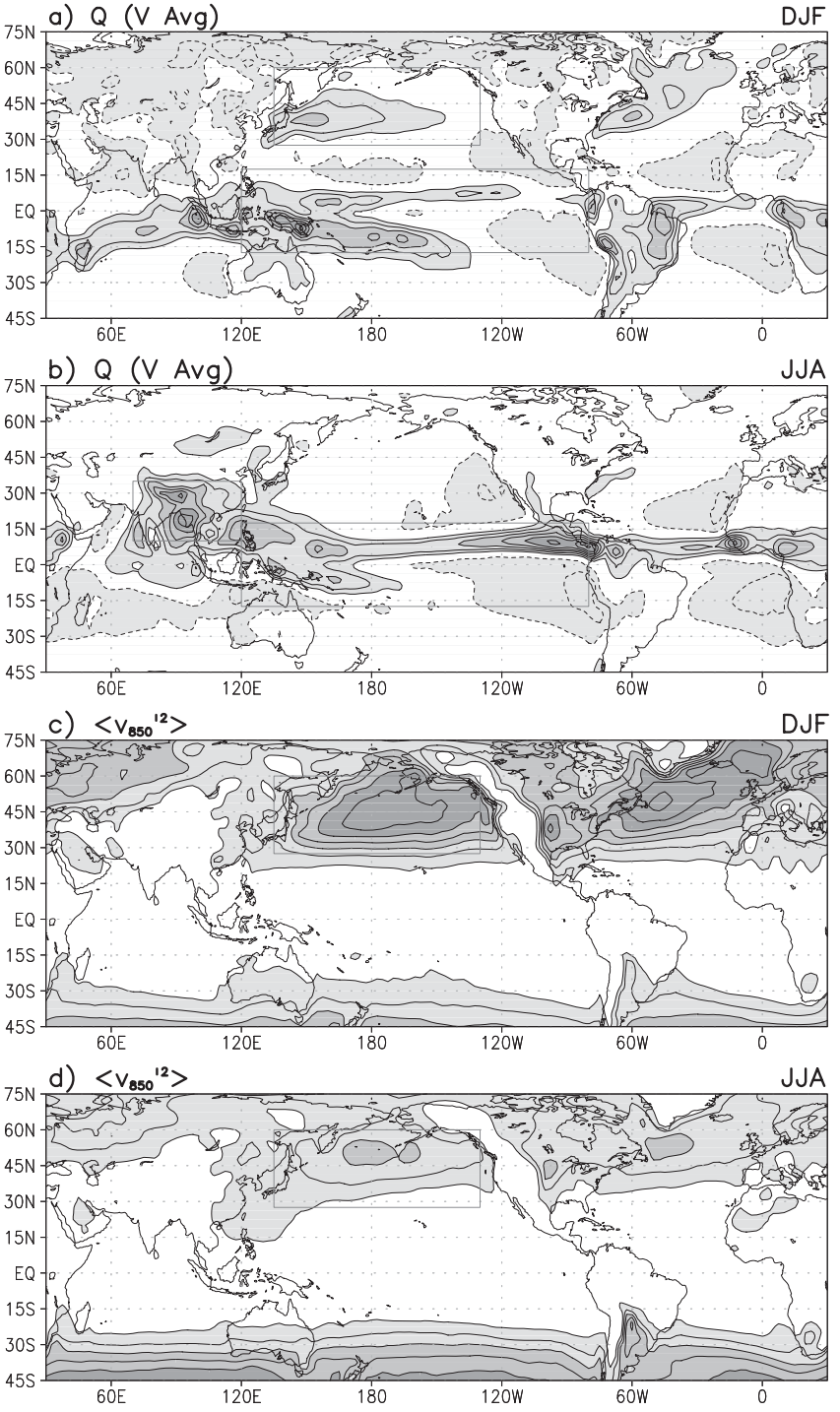

FIG. 8. Vertically averaged ERA-40 diabatic heating in (a) winter (DJF) and (b) summer (JJA) in the 1979–2001 climatology. Heating is residually diagnosed and the surface–125-hPa mass-weighted average is displayed with a 0.75 K day^{-1} interval. The submonthly meridional wind variance at 850 hPa, an indication of transient activity, in (c) winter (DJF) and (d) summer (JJA), with a 15 m^2 s^{-2} interval. Solid (dashed) contours indicate positive (negative) values and the zero contour is omitted in all panels. The superposed rectangles outline three forcing regions whose responses are analyzed in a later section: the Asian monsoon (10°–35°N, 70°–120°E), the ITCZ heating (17.5°S–17.5°N, 120°E–80°W), and the Pacific storm tracks (27.5°–60°N, 135°E–130°W).

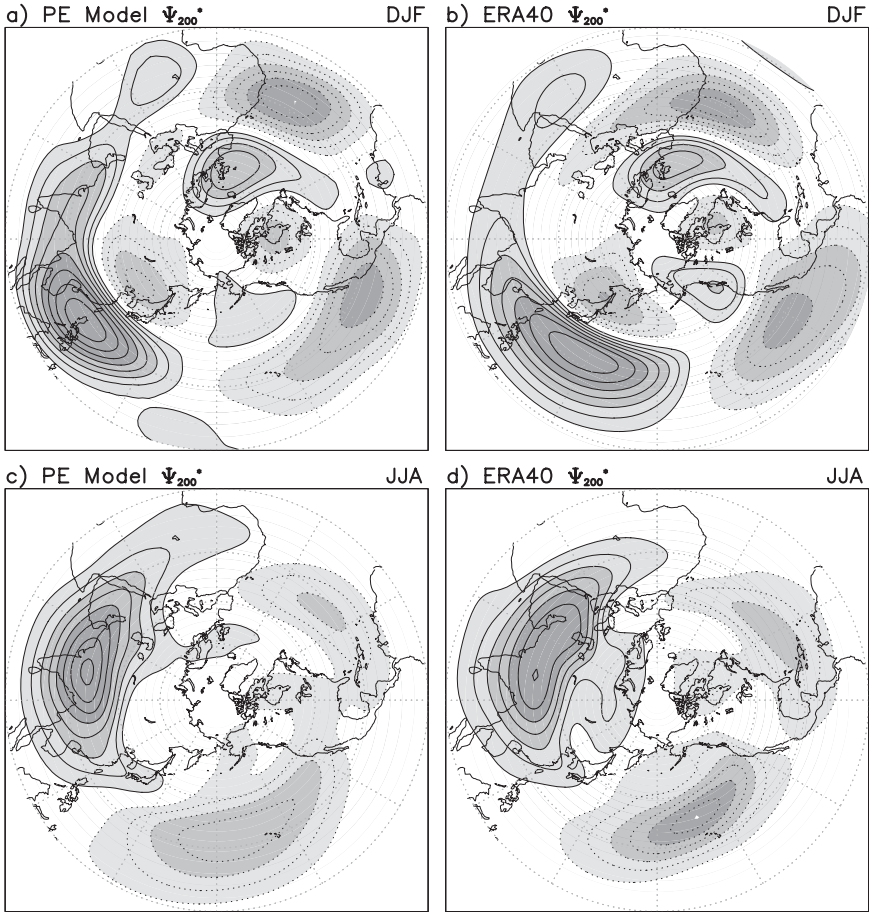

FIG. 9. Diagnostically modeled and observed 200-hPa eddy streamfunction in (a),(b) winter and (c),(d) summer in the 1979–2001 period climatology. The contour interval is 4.0E6 $m^2 s^{-1}$, or ~40 gpm in the midlatitudes. Solid (dashed) contours indicate positive (negative) values. The zero contour is omitted in all panels.

streamfunction is, often, shown instead.) The diagnostic model's inability to represent the blocking of flow by orography on account of the linearized dynamics further contributes to this challenge.

The fidelity of the individual season simulations and the largely acceptable simulation of winter-to-summer SLP development suggests that the diagnostic model meets the prerequisites for conducting a dynamical diagnosis of SLP development.

The analysis begins by displaying the response of the winter-to-summer change in diabatic heating and transient fluxes in Fig. 10c.[15] The SLP response is focused in the extratropical basins (~8 hPa), with the longitudinal position of the Pacific maximum in better accord with observations (Fig. 10a). The Atlantic development is also more realistic. The response forced by heating and transients is of more interest than the full solution as the latter contains a component forced by the surface temperature boundary condition. The boundary condition is introduced into the model from the vertical diffusion of temperature in the PBL. The related model response is considered part of the local feedback as SSTs underneath the SLP anticyclone are not independent of the overlying circulation.

8. Dynamical diagnoses of winter-to-summer SLP development

Atmospheric diabatic heating and transient fluxes account for a substantial portion of the winter-to-summer SLP development in the extratropical Pacific (cf. Fig. 10c). The geographic regions that most influence this seasonal development are identified in this section

[15] The solution forced by orography and surface temperature is first subtracted from the full solution for each season, leading to the component forced by heating and transients alone. The winter-to-summer change in this component is shown in Fig. 10c.

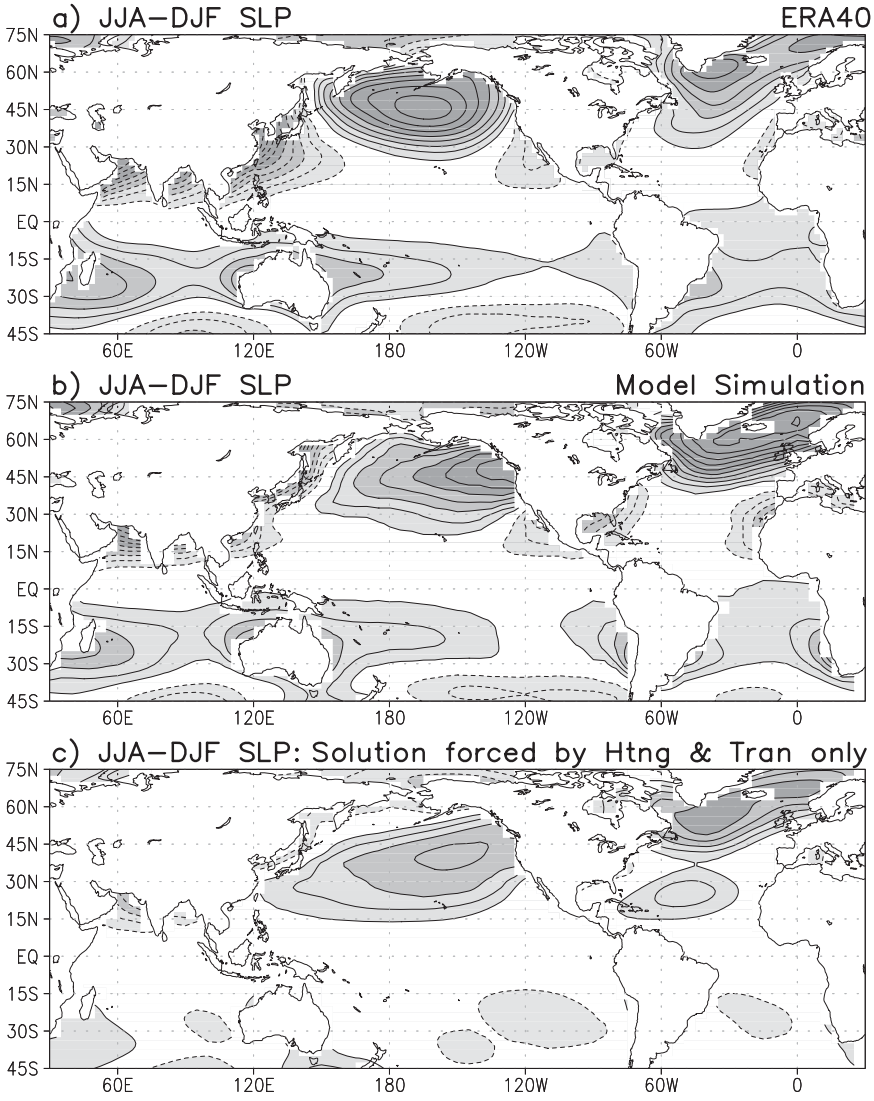

FIG. 10. Diagnostically modeled and observed winter-to-summer *development* in SLP in the 1979–2001 period climatology: (a) ERA-40; (b) diagnostic simulation, from the difference of winter and summer solutions; and (c) simulation component due to changes in 3D diabatic heating and vorticity and thermal transients, i.e., without lower-boundary (orography and surface temperature) influences. The contour interval is 2.0 hPa and solid (dashed) contours indicate positive (negative) values. The zero contour is omitted in all panels, as before.

from diagnostic modeling, with the model's linearity as the basis for the analysis. The forcing regions are marked by rectangles in Fig. 11, which also displays their contribution to SLP development.

The change in forcing over the Asian continent (10°–35°N, 70°–120°E), principally from summer monsoon development, enhances the SLP over the subtropical Pacific (and Atlantic) by 2–3 hPa, as shown in Fig. 11a. The response is similar to that arising from just the summertime forcing, but the winter response (~1 hPa) is not insignificant (neither shown). The impact of the Asian continent on Pacific SLP development is modest though, given the 2–3-hPa response vis-à-vis the ~8 hPa signal being diagnosed (Fig. 10c). Rodwell and Hoskins (2001) assessed the influence of the summer monsoon using an expansive forcing region that includes portions of the western Pacific Warm Pool to the south and the western North Pacific monsoon to the east (see footnote 9). (Even if relevant in summer, such an expansive region will include both tropical and midlatitude phenomena in winter, compromising its suitability in the analysis of SLP development.)

Sea level pressure development attributable to seasonal change in the tropical Pacific (17.5°S–17.5°N,

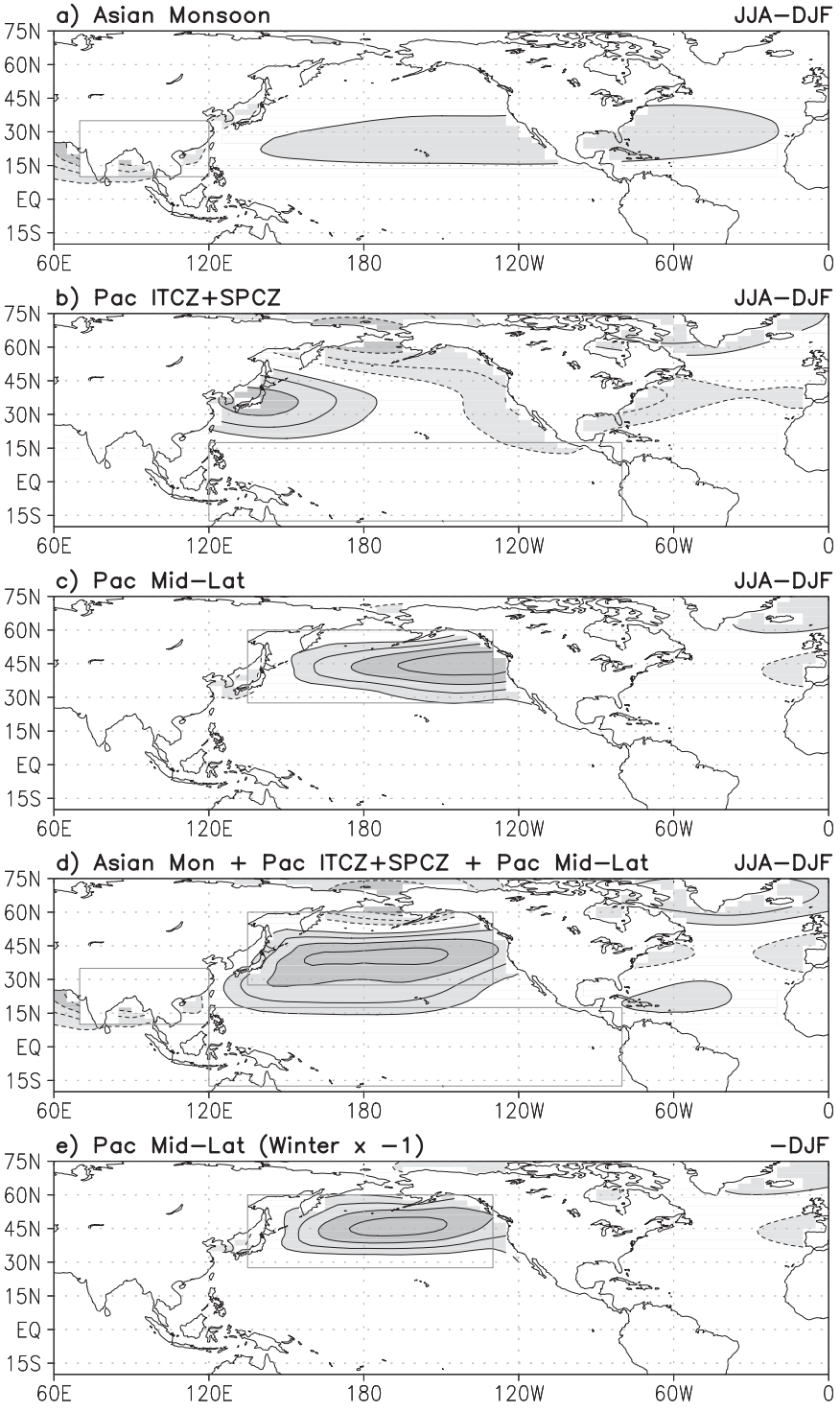

FIG. 11. Dynamical diagnosis of the linearly simulated winter-to-summer SLP *development* forced by seasonal changes in heating and transients (cf. Fig. 10c). Components forced by the JJA–DJF changes in heating and transients over the (a) Asian monsoon region, (b) Pacific ITCZ+SPCZ, (c) Pacific midlatitudes, and (d) sum of the above. (e) SLP forced by winter heating and transients in the Pacific midlatitudes, after multiplication by −1. The contour interval is 2.0 hPa and solid (dashed) contours indicate positive (negative) values in each panel. The zero contour is omitted in all panels, as before.

120°E–80°W) forcing is shown in Fig. 11b. Heating is dominant in the chosen domain (cf. Fig. 8) which fully captures the ITCZ+SPCZ heating in both winter and summer. The SLP development in the subtropics and midlatitudes is substantial (4–6 hPa) and, interestingly, quite similar to the winter response forced from the same region except for the sign (not shown), indicating the strong influence of the abatement of winter tropical forcing on SLP development.[16] Forcing from the tropical Pacific however provides an incomplete account of SLP development as the related response includes low pressure along the North American coast where the response of the global heating and transients is strongly positive (Fig. 10c).

The response forced by the change in heating and transients in the Pacific midlatitudes is shown in Fig. 11c. Both storm-track heating and transients in winter and low-level diabatic cooling in summer contribute to the forcing change. The resulting response is impressive in the central and eastern midlatitude basins. Regardless of the relative roles of winter storm-track abatement and summer radiational cooling, the winter-to-summer change in midlatitude forcing can evidently account for much of the SLP development in the central and eastern basins, that is, for anticyclone buildup. The SLP development generated by the three forcing regions together, that is, the sum of Fig. 11a–c, is shown in Fig. 11d, which compares favorably with the SLP change shown in Fig. 10c, the target for this dynamical diagnosis. The reconstruction attests to the consideration of the key forcing regions in the diagnosis.

The final panel in Fig. 11 depicts the response of winter heating and transients in the Pacific midlatitudes and is multiplied by -1 to facilitate comparison with the SLP development (JJA–DJF) plots. The abatement of winter storm tracks generates a response (Fig. 11e) that is broadly similar to that forced by the winter-to-summer change in heating and transients (Fig. 11c). The modest differences in Fig. 11c and 11e in the subtropics and higher latitudes are indicative of the contribution of summer radiational cooling (from stratus cloud tops in the central and eastern basins) to SLP development.

The role of heating over the North American continent in Pacific SLP development was also assessed, following indications of its importance (Hoskins 1996; Liu et al. 2004; Miyasaka and Nakamura 2005). The winter-to-summer change in heating and transients over the North American continent (20°–60°N, 120°–75°W) generated weak SLP development over the Pacific extratropics, at least, in our analysis (not shown). The SLP response was of the right sign (+) but of weak amplitude (~1 hPa). The response was somewhat more consequential along the Baja California coast, where it lowers SLP.

[16] Tropical forcing in summer is much less influential in the model because it is well embedded in the zonal-mean tropical easterlies (about which the model is linearized). Zonal-mean easterlies occur in winter too but in a much narrower equatorial belt (especially in the NH), allowing winter forcing to be influential.

9. Concluding remarks

This study seeks to advance the understanding of the causes of seasonal SLP variability over the NH ocean basins, in particular, the waxing and waning of the Pacific anticyclone, a majestic feature occupying almost the entire extratropical basin in July. Because of its expanse, perhaps, the Pacific anticyclone has not acquired a different name, unlike its Atlantic counterpart, which is known as the Azores (or Bermuda) high. Sea level pressure is, of course, one of the most analyzed meteorological variables (e.g., Walker and Bliss 1932) but its seasonal variability, as reflected in the summer strength and expanse of the NH anticyclones, has defied understanding because of the timing, which is counterintuitive from the Hadley cell perspective.

A number of studies have sought improved understanding of this counterintuitive evolution since the paradox was eloquently posed by Hoskins (1996). Given the summer vigor of the NH anticyclones, monsoons were implicated. Diagnostic modeling of the summer circulation (e.g., Ting 1994; Rodwell and Hoskins 2001) did show monsoon latent heating to the east and the west of the anticyclone to be important for the summer structure, in addition to local low-level diabatic cooling (of radiative origin), which is of a more feedback than causative nature. Given these dynamical analyses, which are quite robust, one may well ask why the origin of anticyclone seasonality is being revisited in this paper.

The motivation for revisiting the paradoxical evolution of the Pacific anticyclone came from analysis of seasonal SLP variability, especially the structure and magnitude of SLP *change* over 2-month periods, beginning in January (Fig. 3). This straightforward analysis shows the following:

- The winter-to-summer SLP change is *gradual*, consisting of three comparable 2-month changes. Anticyclone buildup leading to the majestic summer structure is thus not confined to the monsoon-onset period (May–July). Waxing and waning of the anticyclone must therefore be due to more than just the onset and demise of the summer monsoons.
- In the build-up phase, positive SLP development is focused in the extratropical basin (northward of the

tropic of Cancer). The tropical–subtropical basin exhibits a modest SLP change, 1–2 hPa, with the monsoon-onset period change being, in fact, negative!

- Tracking the anticyclone's evolution via the 1020-hPa isobar in the full SLP field (physically appealing) confirms that the change in SLP in the tropical and subtropical basins is quite modest.

The evolution of other prominent anticyclones, for example, the Azores (Bermuda) high in the NH and the Mascarene high in the SH, was also examined with the hope that intercomparisons may shed light on their development mechanisms. We found the Azores high and Pacific anticyclone evolutions to be similar, with both exhibiting peak amplitude/expanse in summer. Annual SLP variability in the Atlantic also exhibits large amplitudes in the high latitudes and modest variability in the subtropics. The similarity, despite the absence of an Asian monsoon equivalent to the west, suggests that either a monsoon to the west is inconsequential or the global reach of the Asian monsoon, and/or the significant influence of storm-track abatement in each basin.

The SH anticyclones are found to peak in austral winter, in contrast with the northern ones. This peak-phase timing rules out the SH monsoons and storm tracks as a causative influence; the latter is not surprising, given their subpolar, distant location. The waxing and waning of the SH anticyclones can be accounted for by the Hadley cell's seasonality—in accordance with dynamical intuition that proved incorrect in the NH (due to interference from robust storm track and monsoon influences).

If monsoons cannot be implicated in the summer vigor of the Pacific anticyclone, the paradox that Hoskins posed stands. The paradox is resolved by first noting that it is the weak seasonality of SLP in the tropics–subtropics (Figs. 2–4), rather than perceptions of a large counterintuitive (i.e., positive) signal there (cf. Hoskins 1996), that is perplexing in the context of the striking winter-to-summer weakening of the Hadley cell. [Positive SLP development does occur in summer but well to the north (~45°N), as shown in Figs. 2–4.] The striking seasonality of the Hadley cell is, moreover, shown to arise from (and thus represent) descent variations related to the Asian summer monsoon's onset and demise, consistent with the results of Dima and Wallace (2003). Descent over the central/eastern basins (anticyclone domain), in fact, exhibits far less seasonal variation than is implied by the Hadley cell's striking seasonality along with flawed notions of it being zonally representative, thus, resolving the paradox.

The apparent contradiction between observational findings and modeling analyses on the role of monsoons in anticyclone development arises not because either is flawed, but because the two cannot be directly compared: modeling studies have hitherto targeted the summer circulation itself, not circulation development (cf. Fig. 3), the pertinent target in the context of the summer peaking of anticyclone's strength/expanse. Anticyclone development, especially when gradual, can depend as much on forcing onsets as abatements. This suggests that mechanisms posited for the summer robustness of the NH anticyclones from modeling analyses need to be reaffirmed.

Dynamical diagnosis of circulation development over the Pacific concludes this inquiry. A steady, linear primitive equation model that reasonably simulates the winter-to-summer (JJA–DJF) SLP development when forced by ERA-40-derived diabatic heating and transient fluxes is used to assess the contributions of three forcing regions: the Asian monsoon, the Pacific tropics, and the Pacific midlatitudes. Of the three, the Pacific midlatitudes are the most influential, contributing at least two-thirds of the SLP development signal (6–8 hPa), with the bulk coming from the abatement of winter storm-track heating and transients. The Asian monsoon contribution (2–3 hPa) is dominant in the Pacific (and Atlantic) tropics–subtropics. The response of the Pacific ITCZ+SPCZ heating is confined to the western and far eastern extratropical basins, with the former being influential.

The diagnostic (a posteriori) nature of the modeling assessment and the employed model's simplicity and potential weaknesses (e.g., linearization about a zonal-mean basic state, PBL treatment, etc.) necessitate corroboration of the modeling analysis. For instance, Rodwell and Hoskins (2001) find the blocking of flow by mountain ranges to be important for anticyclone development in the eastern basins, but this effect is not modeled by the linearized dynamics used in this study. On the other hand, the modeling results resonate with the observational findings reported in the first part of the paper.

Acknowledgments. We wish to thank Brian Hoskins and an anonymous reviewer for reading our manuscript and for their constructive suggestions, and Editor Clara Deser for guidance. Sumant Nigam acknowledges NOAA and NSF support through Grants CPPANA17EC1483 and ATM-0649666. Steven Chan was supported by a NASA Earth System Science Fellowship (2004–07).

REFERENCES

Bergeron, T., 1930: Richlinien einer dynamischen klimatologie. *Meteor. Z.,* **47,** 246–262.

Bjerknes, J., 1935: La circulation atmosphérique dans les latitudes sous-tropicales. *Scientia,* **57,** 114–123.

Chan, S. C., and S. Nigam, 2009: Residual diagnosis of diabatic heating from ERA-40 and NCEP reanalyses: Intercomparisons with TRMM. *J. Climate,* **22,** 414–428.

Chang, E. K. M., 1993: Downstream development of baroclinic waves as inferred from regression analysis. *J. Atmos. Sci.,* **50,** 2038–2053.

Chen, P., M. P. Hoerling, and R. M. Dole, 2001: The origin of the subtropical anticyclone. *J. Atmos. Sci.,* **58,** 1827–1835.

Dima, I. M., and J. M. Wallace, 2003: On the seasonality of the Hadley cell. *J. Atmos. Sci.,* **60,** 1522–1527.

Held, I. M., S. W. Lyons, and S. Nigam, 1989: Transients and the extratropical response to El Niño. *J. Atmos. Sci.,* **46,** 163–174.

Hoskins, B. J., 1996: On the existence and strength of the summer subtropical anticyclones. *Bull. Amer. Meteor. Soc.,* **77,** 1287–1291.

——, and P. J. Valdes, 1990: On the existence of storm-tracks. *J. Atmos. Sci.,* **47,** 1854–1864.

——, and ——, 2002: New perspectives on Northern Hemisphere winter storm tracks. *J. Atmos. Sci.,* **59,** 1041–1061.

——, and K. I. Hodges, 2005: A new perspective on Southern Hemisphere storm tracks. *J. Climate,* **18,** 4108–4129.

——, and Coauthors, 1989: Diagnostics of the global atmospheric circulation based on ECMWF analyses 1979–1989. WMO/TD 326, World Meteorological Organization, 217 pp.

Kållberg, P., P. Berrisford, B. J. Hoskins, A. Simmons, S. Uppala, S. Lamy-Thépaut, and R. Hine, 2005: *ERA-40 Atlas.* ERA-40 Project Rep. Series 19, ECMWF, 103 pp.

Karoly, D. J., and B. J. Hoskins, 1982: Three-dimensional propagation of planetary wave. *J. Meteor. Soc. Japan,* **60,** 109–123.

Krishnamurti, T. N., and H. N. Bhalme, 1976: Oscillations of a monsoon system. Part I. Observational aspects. *J. Atmos. Sci.,* **33,** 1937–1954.

Liu, Y., G. Wu, and R. Ren, 2004: Relationship between the subtropical anticyclone and diabatic heating. *J. Climate,* **17,** 682–698.

Miyasaka, T., and H. Nakamura, 2005: Structure and formation mechanisms of the Northern Hemisphere summertime subtropical highs. *J. Climate,* **18,** 5046–5065.

Newell, R. E., J. W. Kidson, D. G. Vincent, and G. J. Boer, 1972: *The General Circulation of the Tropical Atmosphere and Interactions with Extratropical Latitudes.* Vol. 1. The MIT Press, 258 pp.

Nigam, S., 1994: On the dynamical basis for the Asian summer monsoon rainfall–El Niño relationship. *J. Climate,* **7,** 1750–1771.

——, 1997: The annual warm to cold phase transition in the eastern equatorial Pacific: Diagnosis of the role of stratus cloud-top cooling. *J. Climate,* **10,** 2447–2467.

——, and R. S. Lindzen, 1989: The sensitivity of stationary waves to variations in the basic state zone flow. *J. Atmos. Sci.,* **46,** 1746–1768.

——, and A. Ruiz-Barradas, 2006: Seasonal hydroclimate variability over North America in global and regional reanalyses and AMIP simulations: Varied representation. *J. Climate,* **19,** 815–837.

——, C. Chung, and E. DeWeaver, 2000: ENSO diabatic heating in ECMWF and NCEP reanalyses, and NCAR CCM3 simulation. *J. Climate,* **13,** 3152–3171.

Peterson, M., cited 2007: Naming the Pacific. Common-Place, Vol. 5, No. 2, American Antiquarian Society. [Available online at http://www.common-place.org/vol-05/no-02/peterson/index.shtml.]

Petterssen, S., 1940: *Weather Analysis and Forecasting.* McGraw-Hill, 505 pp.

Pierrehumbert, R. T., 1995: Thermostats, radiator fins, and local runaway greenhouse. *J. Atmos. Sci.,* **52,** 1784–1806.

Rodwell, M. J., and B. J. Hoskins, 1996: Monsoons and the dynamics of deserts. *Quart. J. Roy. Meteor. Soc.,* **122,** 1385–1404.

——, and ——, 2001: Subtropical anticyclones and summer monsoons. *J. Climate,* **14,** 3192–3211.

Sardeshmukh, P. D., 1993: The baroclinic χ problem and its application to the diagnosis of atmospheric heating rates. *J. Atmos. Sci.,* **50,** 1099–1112.

Seager, R., R. Murtugudde, A. Clement, A. Gordon, and R. Miller, 2003: Air–sea interaction and the seasonal cycle of the subtropical anticyclones. *J. Climate,* **16,** 1948–1965.

Ting, M., 1994: Maintenance of northern summer stationary waves in a GCM. *J. Atmos. Sci.,* **51,** 3286–3308.

Uppala, S., and Coauthors, 2005: The ERA-40 Re-Analysis. *Quart. J. Roy. Meteor. Soc.,* **131,** 2961–3012.

Walker, G. T., and E. W. Bliss, 1932: World weather V. *Mem. Roy. Meteor. Soc.,* **4,** 53–84.

Xie, P., and P. A. Arkin, 1997: Global precipitation: A 17-year monthly analysis based on gauge observations, satellite estimates, and numerical model outputs. *Bull. Amer. Meteor. Soc.,* **78,** 2539–2558.